ACS OMEGA

Article

Cite This: ACS Omega 2018, 3, 7196−7203

Kinetics, Isotherm, and Thermodynamic Studies of Methylene Blue Adsorption on Polyaniline and Polypyrrole Macro−Nanoparticles Synthesized by C-Dot-Initiated Polymerization

Moorthy Maruthapandi,[†] Vijay Bhooshan Kumar,[†] John H. T. Luong,[‡] and Aharon Gedanken*[,†]

[†]Bar-Ilan Institute for Nanotechnology and Advanced Materials, Department of Chemistry, Bar-Ilan University, Ramat-Gan 52900, Israel

[‡]School of Chemistry, University College Cork, Cork T12 K8AF, Ireland

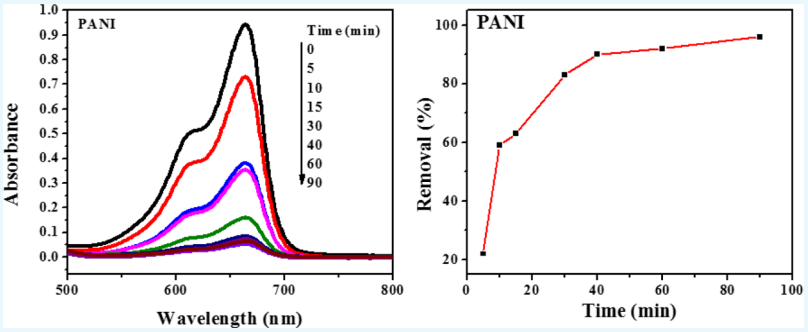

ABSTRACT: This work unraveled kinetics, isotherm, and thermodynamic properties of methylene blue (MB) adsorbed on polyaniline (PANI) and polypyrrole (PPY). The two polymers, PANI and PPY, synthesized by a facile C-dot (CD)-initiated polymerization method have been proven as the effective adsorbent materials to remove MB from wastewater. This dye model is also generally employed as a redox indicator in analytical chemistry and exhibits blue in an oxidizing environment, but it is colorless when exposed to a reducing agent. The effects of temperature, adsorbent amount contact time, and dye concentration were consistently examined. The adsorption capacity of the polymers at 28 °C could reach 19.2 mg/g. The adsorption equilibrium of the dye was attained after 90 and 120 min of contact time with PANI and PPY, respectively. The equilibrium details were well described by Freundlich and Langmuir isotherms. Results showed that PANI and PPY prepared using CD-initiated polymerization are better adsorbents compared to the commercial PANI powder for the removal of MB from water.

1. INTRODUCTION

Polymer materials have attracted significant attention for different applications including dye removal[1−4] and remediation because of their high thermal stability, adsorption capacity, and chemical stability. A recent novel polymerization method of polyaniline (PANI) and polypyrrole (PPY) used carbon dots (CDs) and UV light, avoiding the regular oxidation initiators.[5] In fact, CDs play a major role as an initiator. There are many organic and inorganic dyes that are currently used in industrial leather, plastic, textile, pulp and paper making, pharmaceuticals, cosmetics, and printing.[6] However, despite their beneficial use, such dyes are poisonous and harmful to humans and the environment. Dyes used in these industries must have high photocatalytic and chemical stability; therefore, the biological and biodegradable treatment of these dyes is too difficult. Different types of dyes used by the textile industry are discharged into waste streams, causing a serious problem for the environment.[7] Considering various treatment methods to degrade dyes, the resultant degradation products are still poisonous, teratogenic, and carcinogenic for living organisms. Thus, such unwanted color dyes and their disruption products are also carcinogenic to human beings.[8] Moreover, there are many physical, chemical, and biological techniques used to remove dyes from an aqueous solution.[9] Nevertheless, these methods always show few disadvantages such as energy intensiveness, long time process, high cost, and toxicity.[10] To our knowledge, the adsorption process is an economic, effective, and easily operated process.[11] Several inorganic and organic adsorbent materials have been used to remove dyes from an aqueous solution.[12,13] However, such adsorbent materials always suffer from problems in the separation, forming byproducts and reproduce from wastewater.

Some reports pertain to the adsorption properties of polymer-based nanomaterials such as pyrrole-based materials,[14] PANI nanotubes,[15] polydopamine,[16−18] PANI-based silica composite,[19] nanocrystalline cellulose,[8] and bioadsorbents.[20−25] In this regard, PANI and PPY can be used as adsorbent materials because of their good chemical and thermal stability, good morphologies, low cost, and ease of

Received: March 14, 2018
Accepted: June 18, 2018
Published: July 2, 2018

DOI: 10.1021/acsomega.8b00478
ACS Omega 2018, 3, 7196−7203

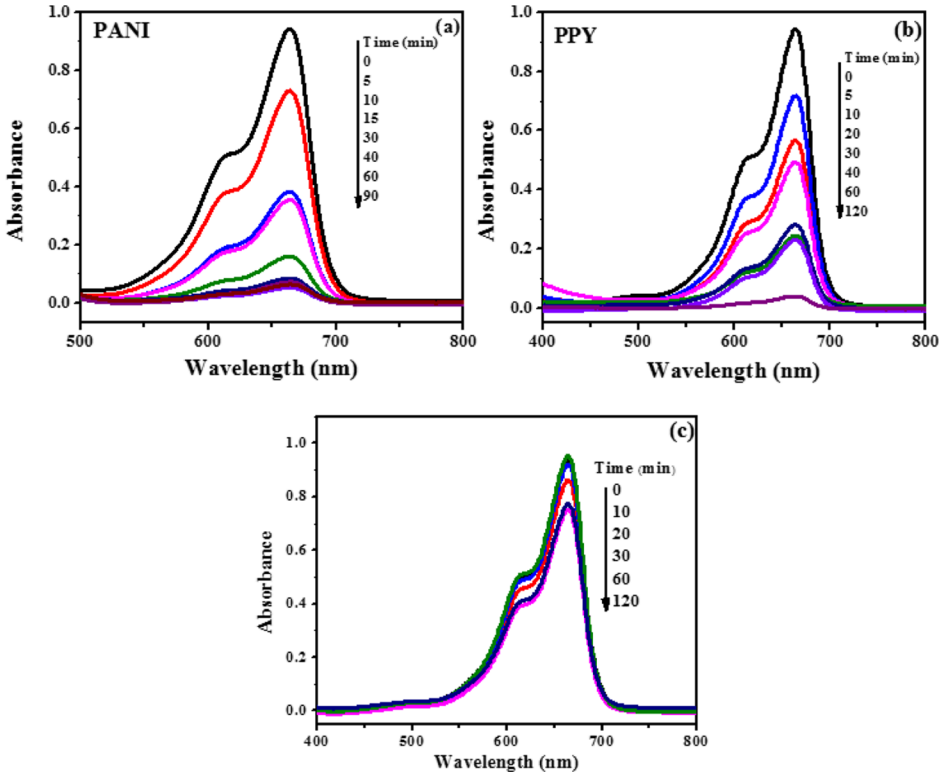

Figure 1. Time-resolved adsorption spectra of the MB dye (20 mL of 50 mg L^{-1}) with 0.05 g of PANI material (a), time-resolved adsorption spectra of MB dye (20 mL of mg L^{-1}) with 0.05 g of PPY (b), and time-resolved adsorption spectra of MB dye (20 mL of mg L^{-1}) with 0.05 g commercial PANI emeraldine salt (c).

synthesis. The adsorption of methylene blue (MB) on PANI and PPY as a working model was conducted under varying adsorption conditions to decipher kinetics, thermodynamics, and isotherms of the adsorption process.

2. RESULTS AND DISCUSSION

2.1. Adsorption of MB by PANI and PPY. The absorbance of MB after the addition of 0.05 g of PANI and PPY to a 50 mg L^{-1} solution of MB as a function of time is depicted in Figure 1a,b. The figure reveals a decrease in the absorbance of MB as a function of time. As shown in Figure 1a, the difference in the adsorption of MB between PANI and PPY is small, except that the concentration of MB is almost completely reduced by PANI in 90 min, compared to 120 min for PPY. In Figure 1c, the addition of 0.05 g of commercial PANI (ES) to 50 mg L^{-1} of MB solution results in no change in the initial absorbance even after 120 min into the experiment.

The explanation for the difference in the adsorption of MB by the commercial PANI and the CD-synthesized polymer is related to the size and shape of the two polymers (Figure 2b,a). The structure of the CD-initiated PANI product reveals a mixture of nanotubes whose diameters are in the 70−500 nm range (Figure 2a) and many flat micron-sized irregular structures. The commercial PANI reveals large clusters (15 μm) built of flat particles of 1−2 μm size (Figure 2b). The highly aggregated structure limits the free surface area for adsorbing molecules, while the long narrow tubes expose a large surface area for adsorbing the MB molecules. The transmission electron microscopy (TEM) image (Figure 2c) of CD-initiated PANI shows that most of the materials are in the form of nanoparticles, and only a few nanotubes of PANI were

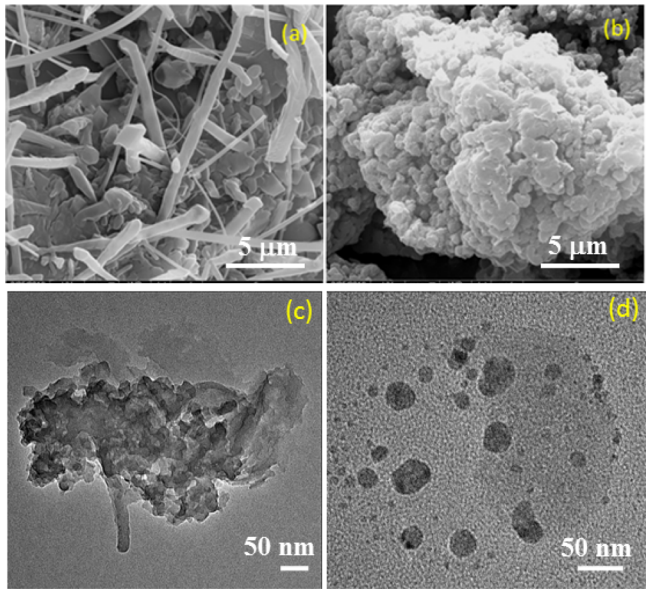

Figure 2. (a) CD-initiated PANI synthesis, (b) commercial PANI, (c) TEM image of CD-initiated PANI synthesis, and (d) TEM image of CD-initiated PPY synthesis.

observed. Figure 2d shows the TEM image of PPY, which shows spherical-shaped nanoparticles 20−60 nm in diameter.

2.2. Adsorption Studies. The MB aqueous solutions were prepared by mixing MB in water and diluted with deionized water to form a series of desired concentrations. The adsorption capacity was calculated using eq 1, where (q) is the amount of MB adsorbed per unit mass of PANI and PPY.

DOI: 10.1021/acsomega.8b00478
ACS Omega 2018, 3, 7196−7203

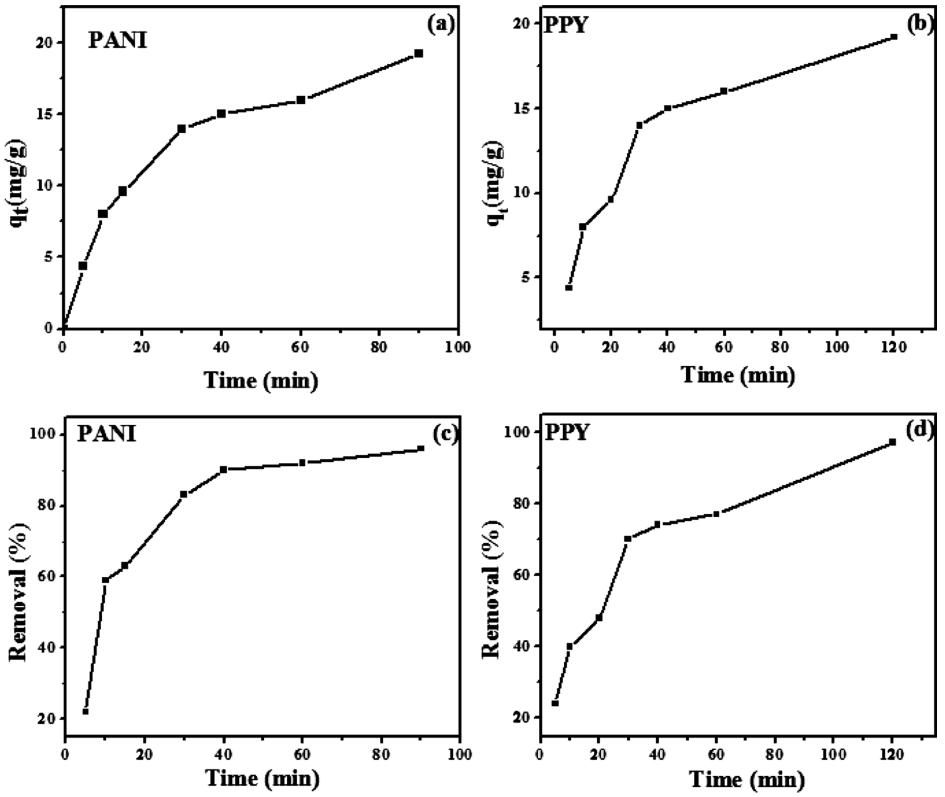

Figure 3. (a,b) Results of the removal of MB as a function of the contact time. The adsorption capacity of MB (50 mg L^{-1}) onto PANI and PPY (0.05 g) (c,d) is found.

The dye removal efficiency (R) was calculated using eqs 1 and 2

$$q = V(C_o - C)/m \quad (1)$$

$$R = 100(C_o - C_t)/C_o \quad (2)$$

where V (L) represents the volume of MB and m (g) is the mass of the adsorbent (PANI and PPY). C_o and C_t (mg L^{-1}) are the initial and final concentrations (after adsorption) of MB solution, respectively.

For the study of adsorption kinetics, 20 mL of the stock solution of MB is added to 0.05 g of PANI or PPY with an initial concentration of 50 mg L^{-1} in a 100 mL beaker at 28 °C until the system reaches the adsorption equilibrium with different time periods. The concentration of MB suspension in supernatant solutions was used to calculate q at equilibrium. The adsorption capacity of MB onto the polymer is represented in Figure 3a,b, and the removal efficiency of MB with the contact time is depicted in Figure 3c,d. The PANI material completely removes MB from the aqueous solution in 90 min, and the MB removal efficiency reaches up to 96%, as shown in Figure 3c, whereas the PPY material removes it in 120 min and the MB removal efficiency reaches up to 97%. This shows that synthesized PANI and PPY materials have superior adsorption properties with respect to the metal oxide system.[26,27]

2.3. Adsorption Mechanism for MB onto PANI. The Fourier-transform infrared (FTIR) spectra of PANI and PANI−MB are shown in Figure 4. The absorption peak of PANI at 3334 cm^{-1} is assigned to the stretching vibration of the amine, and the peak at 1577 cm^{-1} is assigned to the stretching vibration of the aromatic ring. The peak at 1505 cm^{-1} is attributed to the N−H sharing vibration, and the peak at 1340 cm^{-1} is attributed to the C−N stretching vibration. The FTIR spectrum of PANI−MB displays various changes. The intensity of the band at 3334 cm^{-1} of the PANI−MB spectrum is considerably reduced, indicating that the amine plays a major role in the adsorption process. The peak at 1577 cm^{-1} is shifted to a higher frequency and that at 1340 cm^{-1} is shifted to a lower frequency. The peak at 1577 cm^{-1} that is assigned to the aromatic rings is shifted to 1602 cm^{-1} after the adsorption of the MB. These changes may be due to the following reasons. The surface of the adsorbent material exposes the amine groups on the PANI, serving as the adsorption sites for the interaction with MB. Because MB is a planar aromatic molecule and PANI also has many aromatic rings, the $\pi-\pi$ stacking interactions could occur between PANI and MB, displaying the shift of the absorption peak at 1577 cm^{-1}, which is assigned to the aromatic moiety. The electrostatic interactions are the driving forces of the adsorption of cationic MB onto the basic sites of PANI.

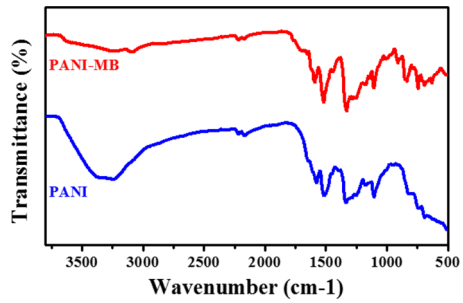

Figure 4. FTIR spectra of PANI and PANI−MB.

DOI: 10.1021/acsomega.8b00478
ACS Omega 2018, 3, 7196−7203

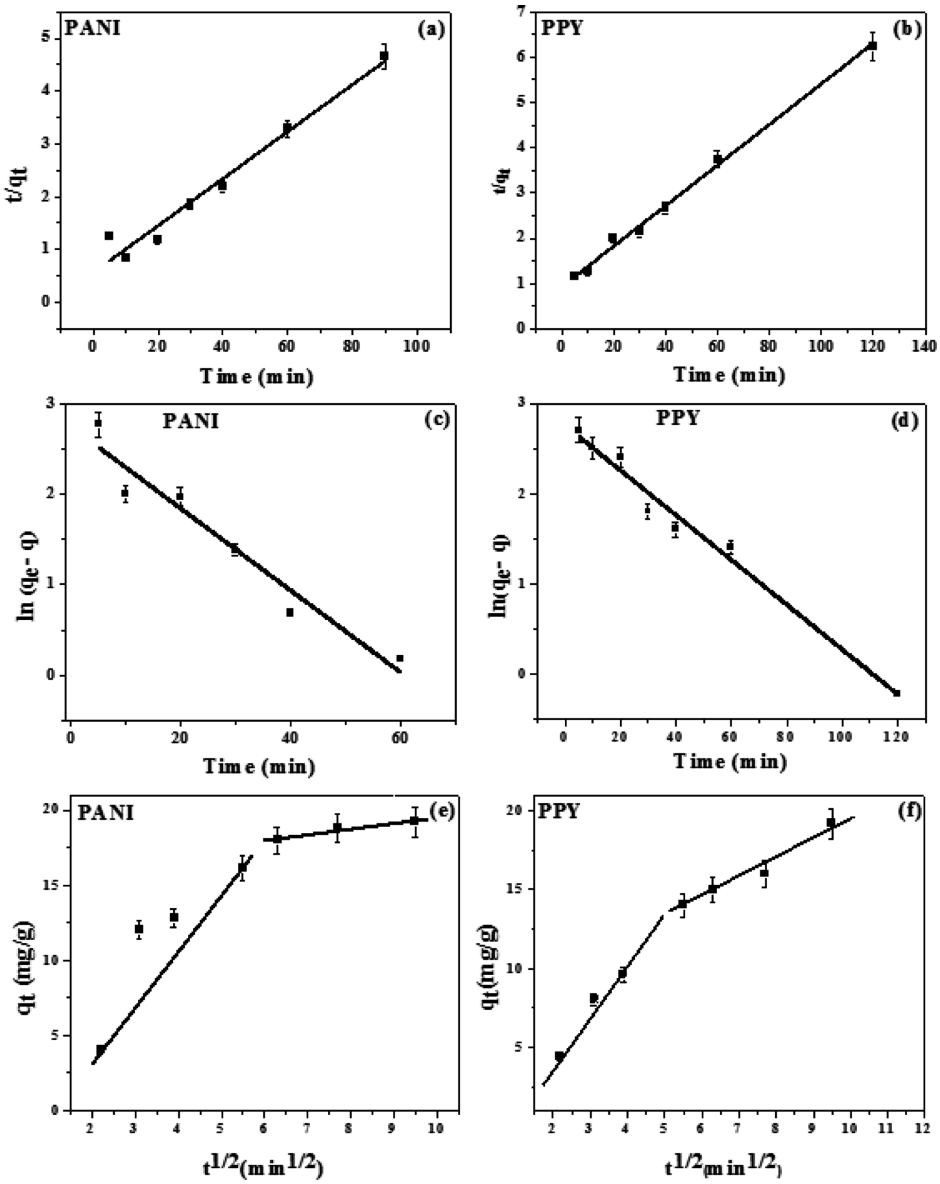

Figure 5. (a,b) Pseudo-first-order model of PANI and PPY, (c,d) pseudo-second-order model of PANI and PPY, and (e,f) intraparticle diffusion kinetic plot of MB on PANI and PPY.

Table 1. Kinetic Model for Adsorption of MB onto PANI and PPY

	model parameters			
models	PANI	R^2	PPY	R^2
pseudo-first order	$q_{e,cal}$ = 18.7 mg/g k_1 = 0.035 min^{-1}	0.93	$q_{e,cal}$ = 16.14 mg/g k_1 = 0.025 min^{-1}	0.97
pseudo-second order	$q_{e,cal}$ = 22.2 mg/g k_1 = 0.0152 g mg^{-1} $min^{-1/2}$	0.96	$q_{e,cal}$ = 20.8 mg/g k_2 = 0.0096 g mg^{-1} $min^{-1/2}$	0.99
intraparticle diffusion	C_1 = 1.77 mg/g K_{i1} = 2.33 mg/g $min^{1/2}$	0.93	C_1 = 2 mg/g K_{i1} = 1.90 mg/g $min^{1/2}$	0.91
	C_2 = 15.9 mg/g K_{i2} = 0.34 mg/g $min^{1/2}$	0.99	C_2 = 9.2 mg/g K_{i2} = 1.18 mg/g $min^{1/2}$	0.97

2.4. Adsorption Kinetics. Kinetics studies on the adsorption of MB were conducted at 28 °C. Because the kinetics information can provide knowledge on the mechanism and the adsorption rate, carrying out all the experiments at a fixed temperature is essential. Figure 5a,b and c,d shows the pseudo-first- and −second-order kinetics models for the adsorption process of MB on PANI and PPY. Both models in linear forms can be presented as follows

$$\ln(q_e - q_t) = \ln(q_e) - k_1 t \quad (3)$$

DOI: 10.1021/acsomega.8b00478
ACS Omega 2018, 3, 7196−7203

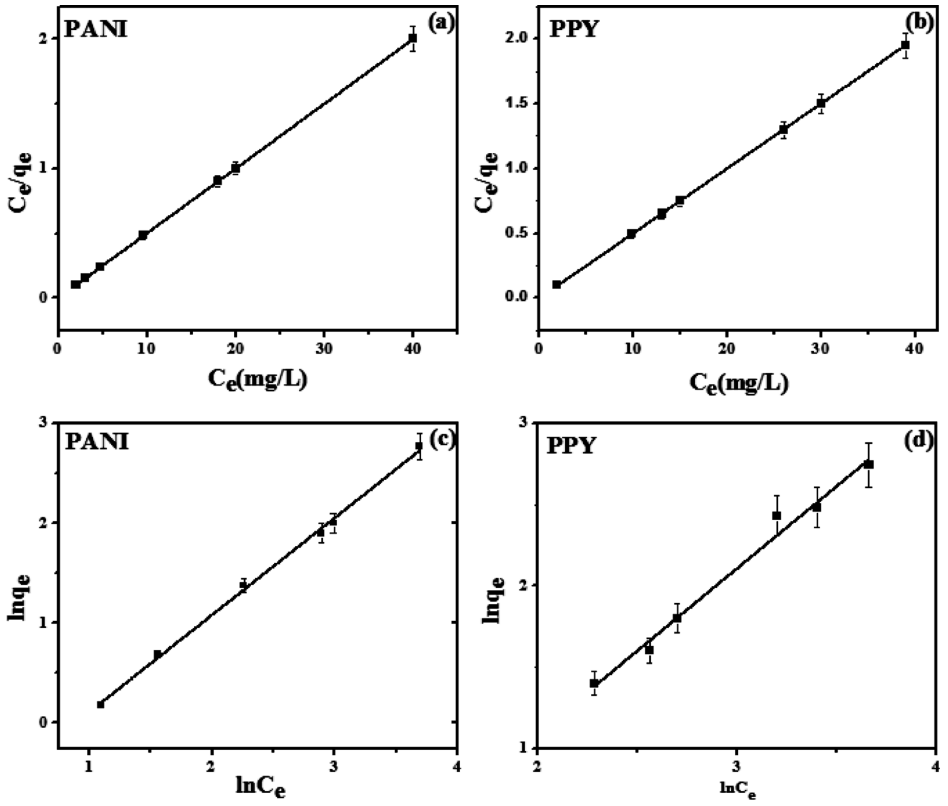

Figure 6. (a,b) Langmuir and (c,d) Freundlich isotherm models for the adsorption of MB onto PANI and PPY.

$$\frac{t}{q_t} = \frac{1}{k_2 q_e^{\,2}} + \frac{t}{q_e} \tag{4}$$

where q_t and q_e mg/g represent the amount of MB (adsorbed at equilibrium), and k_1 (min^{-1}) is the rate constant of the pseudo-first-order model, and k_2 (g mg^{-1} min^{-1}) is the pseudo-second-order model rate constant. The kinetic parameters such as k_1, k_2, correlation coefficients, and calculated $q_{e,cal}$ values are resolved by a linear equation, as shown in Table 1. The $q_{e,cal}$ values of both models are in agreement with the experimental data, where q_e (18.7 mg/g) is for PANI and q_e (16.1 mg/g) for PPY.

The adsorption process is also studied using the Weber and Morris intraparticle diffusion model. In this model, if intraparticle diffusion is the rate-controlling factor, the uptake of the adsorbate varies with the square root of adsorption time. The diffusion model is revealed in eq 5.

$$q_t = k_i t^{1/2} + C \tag{5}$$

The adsorption steps are related to the intercept, which represents the intercept of C (mg/g), and k_i (mg/g $min^{-1/2}$) is the diffusion rate constant. Figure 5e,f shows a multilinear plot of the intraparticle diffusion process of the MB adsorption process on PANI and PPY. Figure 5 indicates two steps that take place during the adsorption process. The first stage indicates the film diffusion model, which is the diffusion of MB from the solution to the external surface of PANI and PPY, and the second step can be attributed to the intraparticle diffusion stage because of the gradual adsorption on the surface of PANI and PPY. As shown in Figure 5e,f, the slope (k_i) of the intraparticle diffusion stage is smaller than that of the film diffusion stage. This result indicates that the intraparticle diffusion stage is a gradual process. The high values of C indicate that the additional mass transfer of MB molecules onto PANI and PPY is significant in the sorption method and occurs in the initial adsorption.

2.5. Adsorption Isotherms. The models of the adsorption isotherms are investigated to provide the detailed facts about the surface adsorbent material properties of the polymers and the adsorption nature. The dynamic concept of adsorption equilibrium is found as soon as the rate of the dye adsorption process is equal to the desorption rate. The observed data of methylene adsorption onto PANI and PPY are fitted to the Freundlich and Langmuir models (Figures 6a–d). In the Langmuir model, the adsorption occurs on a monolayer in all adsorption sites because the adsorbent surface is homogeneous.[16] In contrast, the Freundlich adsorption assumes that the multilayer adsorption process is localized to a heterogeneous surface. The linear equations of the two models are presented as follows

$$\frac{C_e}{q_e} = \frac{1}{q_0 K_L} + \frac{1}{q_0 C_e} \tag{6}$$

$$\ln q_e = \ln K_F + \frac{1}{n C_e} \tag{7}$$

where q_0 (mg/g) and K_L (L/mg) are the Langmuir constants in adsorption capacity and adsorption rate, respectively. In the case of the Freundlich adsorption isotherm, n and K_F are the constants. The Langmuir and Freundlich isotherms of PANI and PPY are shown in Figure 6. The values of K_L, q_0, K_F, and n are determined from the isotherms and the values are shown in Table 2. The R^2 value of the Freundlich and Langmuir model is 1 and 0.98, respectively, validating their applicability. The monolayer adsorption value determined from the Langmuir

DOI: 10.1021/acsomega.8b00478
ACS Omega 2018, 3, 7196−7203

Table 2. Adsorption Isotherms

	PANI	R^2	PPY	R^2
Langmuir adsorption isotherm	q_0 = 19.67 mg/g	1	q_0 = 19.96 mg/g	1
	K_L = 0.214 L/mg		K_L = 0.15 L/mg	
Freundlich adsorption isotherm	n = 1.03 mg/g	1	n = 1.185 mg/g	0.98
	K_F = 2.1 L/mg		K_F = 1.2 L/mg	

isotherm is 19.67 (mg/g) for PANI and 19.96 (mg/g) for PPY, which is in agreement with the experimental data (19 mg/g). These results indicate that the adsorption of MB onto PANI and PPY follows the isotherms models.

The adsorption feasibility is evaluated by the Langmuir isotherm separation factor (R_L). It is calculated using eq 8.

$$R_L = \frac{1}{1 + bC_o} \tag{8}$$

where K_L (L/mg) is the Langmuir constant and C_o (mg L^{-1}) is the initial MB concentration. The results of R_L signify the type of the isotherm; favorable ($0 < R_L < 1$), irreversible ($R_L = 0$), unfavorable ($R_L > 1$), and linear ($R_L = 1$). The determined R_L value of MB adsorption onto PANI and PPY is 0.285 and 0.266, respectively, indicating a favorable adsorption isotherm.

2.6. Thermodynamic Analysis. The temperature studies of the MB adsorption process are shown in Figure 7. The experiments were measured using 50 mg of PANI or PPY in 20 mL of the initial concentration of MB at different temperatures (20−50 °C), with a fixed contact time of 40 min. The removal efficiency of MB increases when the temperature is increased to 50 °C. The measurements require that the adsorption process of MB on PANI and PPY is preferred at higher temperatures within the temperature range that both PANI and PPY can be judged as a highly efficient adsorbent material to remove MB from water. This result can be ascribed to the evidence that there will be many adsorption sites for MB at higher temperatures. The basic thermodynamic parameters of enthalpy (ΔH^0), entropy (ΔS^0), and Gibbs free energy (ΔG^0) for the MB adsorption process were calculated by using the Langmuir isotherm using the following equations.[17]

$$\Delta G^0 = -RT \ln(K_L) \tag{9}$$

$$\ln(K_L) = \frac{\Delta S^0}{R} - \frac{\Delta H^0}{RT} \tag{10}$$

where R is the universal gas constant (8.314 J/mol K), T is the system temperature (K), and K_L is the Langmuir equilibrium constant (L/mol). The entropy and enthalpy change are determined from van't Hoff plots of $\ln(K_L)$ versus $1/T$ (Figure 7b). All thermodynamic parameters are shown in Table 3.

Table 3. Thermodynamic Parameters

	T (K)	ΔG^0 (kJ/mol)	ΔH^0 (kJ/mol)	ΔS^0 (J/mol K)
PANI	293, 303, 313, 323	−6.6, −6.8, −7.4, −8.1	17	120
PPY	293, 303, 313, 323	−5.8, −6.4, −6.8, −7.7	17.2	112

The negative ΔG^0 values of PANI and PPY (−6.6, −6.8, −7.4, −8.1 and −5.8, −6.4, −6.8, −7.7 at 293, 303, 313, and 323) confirm that the adsorption process is spontaneous in nature and is also feasible.[16] The positive ΔH^0 values of PANI and PPY are 17 and 17.2 kJ/mol, which suggest that the MB adsorption process is endothermic, which is consistent with the effect of temperature. The positive ΔS^0 values of PANI and PPY, 120 and 112 (J/mol K), depicted some structural changes in the polymer and MB, increasing the randomness at the solid−liquid interface during the adsorption process.

3. CONCLUSIONS

Micrometric and nanometric particles of PANI and PPY were prepared using a one-step CD-mediated polymerization reaction. These polymers were examined for kinetic studies on MB adsorption. The results demonstrated that MB adsorption depends on the initial concentration, contact time, and temperature. In the kinetics studies, the adsorption equilibrium data were well fitted with the pseudo-first-order and -second-order Langmuir and Freundlich isotherms, respectively. Weber's intraparticle diffusion studies determined two-stage steps that took place while the adsorption process occurred, and it was not the rate-determining step. The thermodynamic studies suggested that the adsorption of MB onto PANI and PPY was spontaneous (ΔG^0; −6.8 and −6.4 at 303 K) and endothermic (ΔH^0: 17 and 17.2 kJ/mol). The adsorbent capacities of facile CD-initiated polymers of PANI and PPY were 19.2 and 19.31 mg/g, compared to 5.01 and 5.7 mg/g for the PANI base[15] and the PANI/silica composite,

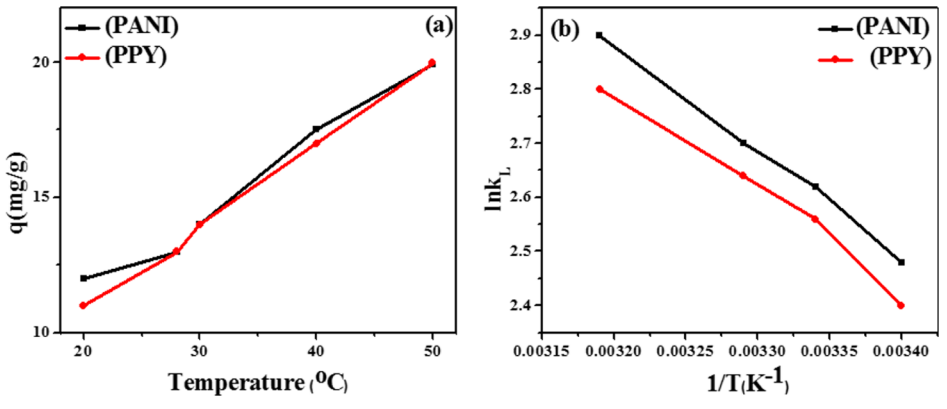

Figure 7. (a) Temperature studies on the MB adsorption onto PANI and PPY and (b) van't Hoff for thermodynamic parameters.

DOI: 10.1021/acsomega.8b00478
ACS Omega 2018, 3, 7196−7203

respectively.[19] Thus, CD-initiated polymers of PANI and PPY are good adsorbent materials compared to the PANI base and the PANI/silica composite for the removal of MB from aqueous solution.

4. EXPERIMENTAL SECTION

4.1. Chemicals. Polyethylene glycol (PEG)-400, nitric acid, pyrrole, aniline, MB, and PANI were purchased from Sigma-Aldrich, Israel.

4.2. Preparation of CDs. The preparation of water-soluble CDs was achieved via a modified sonochemical method using PEG-400, as described previously.[28] Briefly, 30 mL of PEG-400 was poured into a 100 mL beaker and incubated in an oil bath at 70 °C. The tip of an ultrasonic transducer was dipped in the PEG and sonicated for 3 h with 65% amplitude.

4.3. Synthesis of PANI and PPY. The syntheses of PANI and PPY followed our previous report.[5] Aniline (1 g) was mixed in 30 mL of 1.5 M nitric acid in a 100 mL beaker to start the oxidation at room temperature (RT). After the addition of CDs (3 mL), the resulting solution was subject to UV irradiation for 1 week. The brown powder was collected using filtration, washed many times with water, and dried at RT.[5] Similarly, pyrrole (1.0 g) was mixed in 30 mL of 1 M nitric acid in a 100 mL beaker at RT. CD solution (3 mL) was added. The polymerization reaction was carried out by illumination with UV for 3 days, resulting in a brown powder. The powder was collected using filtration, washed many times with water, and dried at RT.[5]

4.4. MB Adsorption. The stock solution was prepared as follows: 50 mg of MB was dissolved in 1 L of distilled water. The concentration (initial and final) of MB solutions was analyzed by UV−visible spectroscopy. The kinetic measurements were studied in the following condition: 28 °C, a fixed concentration of MB, and neutral pH (6.5) without any external adjustment. MB (20 mL) of various concentrations was added to 0.05 g of PPY and PANI and stirred at 1600 rpm by a magnetic stirrer for different contact times. The suspensions of the adsorbent and MB solutions were separated by a syringe. The concentrations of the MB suspension of the supernatant solution after different time periods (5−120 min) were measured by a UV−visible spectrophotometer. The chemical structures of PANI and PPY are depicted in Scheme 1.

4.5. Analytical Technique. The polymer materials were characterized by various analytical techniques—FTIR spectra, ^{13}C solid-state NMR spectra, thermogravimetric analysis, and scanning electron microscopy. The results of all these characterization methods are already reported in ref 5. UV−visible spectroscopic analyses were conducted at a maximum wavelength of 665 nm of the absorption MB to determine the concentration of MB based on a prepared absorption curve of MB. UV−visible spectra of MB adsorption onto PANI and PPY were analyzed using a Cary 100 spectrophotometer (Varian) operated by Lab Sphere software.

Scheme 1. Possible Structure for (a) PANI and (b) PPY

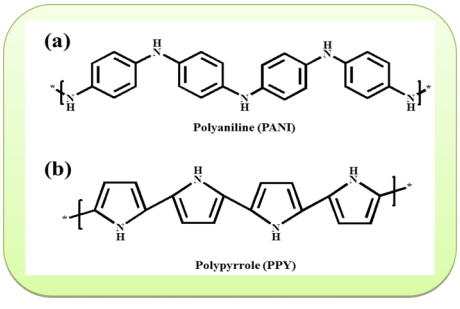

AUTHOR INFORMATION

Corresponding Author

*E-mail: gedanken@mail.biu.ac.il. Phone: +972-3-5318315. Fax: +972-3-7384053 (A.G.).

ORCID

Vijay Bhooshan Kumar: 0000-0001-7899-1463

Aharon Gedanken: 0000-0002-1243-2957

Notes

The authors declare no competing financial interest.

ACKNOWLEDGMENTS

We would like to thank Michal Keren for the solid-state NMR spectrum analysis, carried out in the Chemistry Department at Bar-Ilan University, Israel.

REFERENCES

(1) Mahmoodi, N. M.; Najafi, F.; Khorramfar, S.; Amini, F.; Arami, M. Synthesis, Characterization and Dye Removal Ability of High Capacity Polymeric Adsorbent: Polyaminoimide Homopolymer. *J. Hazard. Mater.* **2011**, *198*, 87−94.

(2) Crini, G.; Badot, P.-M. Application of Chitosan, a Natural Aminopolysaccharide, for Dye Removal from Aqueous Solutions by Adsorption Processes Using Batch Studies: A Review of Recent Literature. *Prog. Polym. Sci.* **2008**, *33*, 399−447.

(3) Crini, G. Kinetic and Equilibrium Studies on the Removal of Cationic Dyes from Aqueous Solution by Adsorption onto a Cyclodextrin Polymer. *Dyes Pigm.* **2008**, *77*, 415−426.

(4) Huang, Q.; Liu, M.; Chen, J.; Wan, Q.; Tian, J.; Huang, L.; Jiang, R.; Wen, Y.; Zhang, X.; Wei, Y. Facile preparation of MoS 2 based polymer composites via mussel inspired chemistry and their high efficiency for removal of organic dyes. *Appl. Surf. Sci.* **2017**, *419*, 35−44.

(5) Moorthy, M.; Kumar, V. B.; Porat, Z.; Gedanken, A. Novel Polymerization of Aniline and Pyrrole by Carbon Dots. *New J. Chem.* **2018**, *42*, 535−540.

(6) Ghanizadeh, G.; Asgari, G. Adsorption Kinetics and Isotherm of Methylene Blue and Its Removal from Aqueous Solution Using Bone Charcoal. *React. Kinet., Mech. Catal.* **2011**, *102*, 127−142.

(7) He, X.; Male, K. B.; Nesterenko, P. N.; Brabazon, D.; Paull, B.; Luong, J. H. T. Adsorption and Desorption of Methylene Blue on Porous Carbon Monoliths and Nanocrystalline Cellulose. *ACS Appl. Mater. Interfaces* **2013**, *5*, 8796−8804.

(8) Ratna; Padhi, B. S. Pollution due to Synthetic Dyes Toxicity & Carcinogenicity Studies and Remediation. *Int. J. Environ. Sci.* **2012**, *3*, 940−955.

(9) Madrakian, T.; Afkhami, A.; Ahmadi, M.; Bagheri, H. Removal of Some Cationic Dyes from Aqueous Solutions Using Magnetic-Modified Multi-Walled Carbon Nanotubes. *J. Hazard. Mater.* **2011**, *196*, 109−114.

(10) Sajab, M. S.; Chia, C. H.; Zakaria, S.; Khiew, P. S. Cationic and Anionic Modifications of Oil Palm Empty Fruit Bunch Fibers for the Removal of Dyes from Aqueous Solutions. *Bioresour. Technol.* **2013**, *128*, 571−577.

(11) Wang, S.; Boyjoo, Y.; Choueib, A.; Zhu, Z. H. Removal of Dyes from Aqueous Solution Using Fly Ash and Red Mud. *Water Res.* **2005**, *39*, 129−138.

(12) Jain, A. K.; Gupta, V. K.; Bhatnagar, A.; Suhas. A Comparative Study of Adsorbents Prepared from Industrial Wastes for Removal of Dyes. *Sep. Sci. Technol.* **2003**, *38*, 463−481.

DOI: 10.1021/acsomega.8b00478
ACS Omega 2018, 3, 7196−7203

(13) Bello, O. S.; Adegoke, K. A.; Olaniyan, A. A.; Abdulazeez, H. Dye Adsorption Using Biomass Wastes and Natural Adsorbents: Overview and Future Prospects. *Desalin. Water Treat.* **2015**, *53*, 1292−1315.
(14) Li, J.; Feng, J.; Yan, W. Excellent adsorption and desorption characteristics of polypyrrole/TiO2 composite for Methylene Blue. *Appl. Surf. Sci.* **2013**, *279*, 400−408.
(15) Ayad, M. M.; El-Nasr, A. A. Adsorption of Cationic Dye (Methylene Blue) from Water Using Polyaniline Nanotubes Base. *J. Phys. Chem. C* **2010**, *114*, 14377−14383.
(16) Fu, J.; Chen, Z.; Wang, M.; Liu, S.; Zhang, J.; Zhang, J.; Han, R.; Xu, Q. Adsorption of Methylene Blue by a High-Efficiency Adsorbent (Polydopamine Microspheres): Kinetics, Isotherm, Thermodynamics and Mechanism Analysis. *Chem. Eng. J.* **2015**, *259*, 53−61.
(17) Fu, J.; Xin, Q.; Wu, X.; Chen, Z.; Yan, Y.; Liu, S.; Wang, M.; Xu, Q. Selective Adsorption and Separation of Organic Dyes from Aqueous Solution on Polydopamine Microspheres. *J. Colloid Interface Sci.* **2016**, *461*, 292−304.
(18) Wang, K.; Fu, J.; Wang, S.; Gao, M.; Zhu, J.; Wang, Z.; Xu, Q. Polydopamine-Coated Magnetic Nanochains as Efficient Dye Adsorbent with Good Recyclability and Magnetic Separability. *J. Colloid Interface Sci.* **2018**, *516*, 263−273.
(19) Ayad, M. M.; Abu El-Nasr, A.; Stejskal, J. Kinetics and Isotherm Studies of Methylene Blue Adsorption onto Polyaniline Nanotubes Base/silica Composite. *J. Ind. Eng. Chem.* **2012**, *18*, 1964−1969.
(20) Kumar, V. B.; Porat, Z.; Gedanken, A. Facile One-Step Sonochemical Synthesis of Ultrafine and Stable Fluorescent C-Dots. *Ultrason. Sonochem.* **2016**, *28*, 367−375.
(21) Salleh, M. A. M.; Mahmoud, D. K.; Karim, W. A. W. A.; Idris, A. Cationic and Anionic Dye Adsorption By Agricultural Solid Waste:a Comprehnsive Veiw. *Desalination* **2011**, *280*, 1−13.
(22) Srinivasan, A.; Viraraghavan, T. Decolorization of Dye Wastewaters by Biosorbents: A Review. *J. Environ. Manage.* **2010**, *91*, 1915−1929.
(23) Salleh, M. A. M.; Mahmoud, D. K.; Karim, W. A. W. A.; Idris, A. Cationic and Anionic Dye Adsorption by Agricultural Solid Wastes: A Comprehensive Review. *Desalination* **2011**, *280*, 1−13.
(24) Wan Ngah, W. S.; Teong, L. C.; Hanafiah, M. A. K. M. Adsorption of Dyes and Heavy Metal Ions by Chitosan Composites: A Review. *Carbohydr. Polym.* **2011**, *83*, 1446−1456.
(25) Dawood, S.; Sen, T. K. Removal of Anionic Dye Congo Red from Aqueous Solution by Raw Pine and Acid-Treated Pine Cone Powder as Adsorbent: Equilibrium, Thermodynamic, Kinetics, Mechanism and Process Design. *Water Res.* **2012**, *46*, 1933−1946.
(26) Liu, Q.; Ai, L.; Jiang, J. MXene-Derived TiO2@C/g-C3N4 Heterojunctions for Highly Efficient Nitrogen Photofixation. *J. Mater. Chem. A* **2018**, *6*, 4102−4110.
(27) Liu, Q.; Zeng, C.; Ai, L.; Hao, Z.; Jiang, J. Boosting Visible Light Photoreactivity of Photoactive Metal-Organic Framework: Designed Plasmonic Z-Scheme Ag/AgCl@MIL-53-Fe. *Appl. Catal., B* **2018**, *224*, 38−45.
(28) Kumar, V. B.; Porat, Z.; Gedanken, A. Facile One-Step Sonochemical Synthesis of Ultrafine and Stable Fluorescent C-Dots. *Ultrason. Sonochem.* **2016**, *28*, 367−375.

DOI: 10.1021/acsomega.8b00478
ACS Omega 2018, 3, 7196−7203